JOURNAL OF SPACECRAFT AND ROCKETS
Vol. 31, No. 3, May–June 1994

Solar Pressure Disturbance on GSTAR and SPACENET Satellites

S. A. Parvez*
GTE Spacenet Corporation, McLean, Virginia 22102

In the geosynchronous orbit, the solar pressure is the primary source of environmental attitude disturbance on the GSTAR and SPACENET satellites. These disturbances are countered by the momentum wheel for the pitch torque, and by the magnetic torquers for the roll and yaw torque. In addition, the north and south solar arrays are differentially slewed to provide an inertially fixed torque to augment the magnetic torquers. This paper attempts to estimate the actual solar pressure torque on the GSTAR I and the SPACENET I satellites at different times of the year. This is obtained by analyzing the on-orbit performance of the momentum wheels and the duty cycles of the magnetic torquers. This paper serves two purposes. Firstly, it estimates the actual solar disturbance torque on satellites in geosynchronous orbit, thereby providing empirical data that can be used for satellite operations. Typically, this information can be used for optimally scheduling some stationkeeping maneuvers, as well as for using solar arrays to augment attitude control operations. Secondly, this data can be used by the designers/manufacturers of satellites to validate their solar pressure disturbance models that are used to design the attitude control system.

Nomenclature

A = diurnal field coefficient
A_r = area exposed to solar radiation, ft^2
B, $\boldsymbol{B}$ = local geomagnetic field ($R_m \cos i_m$), vector, webers/m^2
F = solar pressure force, lbf
H, $\boldsymbol{H}$ = spacecraft momentum magnitude, vector, in-lb-s
i_m = inclination of the Earth's magnetic dipole (11.4 deg)
k_i = disturbance torque coefficients
M, $\boldsymbol{M}$ = control dipole moment magnitude, vector, atm^2
n = unit vector inward normal to an illuminated surface
P_n = solar pressure normal to a surface
P_0 = solar radiation pressure, 9.72×10^{-8} lbf/ft^2
R_m = magnetic field constant, (1.066×10^{-7} weber/m^2)
r = vector from origin to surface dA
r_c = vector from same origin to the center of rotation
s = unit vector in direction of sun rays
T_i = roll/yaw torque coefficients
T_0 = $MB \cos \alpha_s + k_0$
T_1 = $k_1 \sin \beta_o - MBA \cos \alpha_s \cos \beta_o$
T_2 = $k_1 \cos \beta_o + MBA \cos \alpha_s \sin \beta_o$
T_3 = $MB \sin \alpha_s + k_2$
T_4 = $(k_3 - MBA \sin \alpha_s) \cos \beta_o$
T_5 = $-(k_3 - MBA \sin \alpha_s) \sin \beta_o$
t = inward unit vector normal to a surface
α = absorptivity of a surface
α_s = dipole skew angle, deg
β_o = orbit o'clock angle, deg
γ = array offset, degrees ahead of sun
δ = angle by which north array is ahead of south array, deg
ϵ_ϕ = roll threshold (deadband) for control torquing, deg
θ = propeller torque phase angle with sun line, deg
ρ_d = diffuse reflectivity of a surface
ρ_s = specular reflectivity of a surface
σ = incidence angle of sun rays, deg
τ_p = propeller torque, in-lbf
ϕ = roll attitude angle, deg
ψ = yaw attitude angle, deg
Ω = spacecraft station relative to the ascending node of the geomagnetic equator, deg
ω = angular velocity vector relative to inertial space (rad/s)
ω_0 = spacecraft orbital rate, 7.29×10^{-5} rad/s

Received Nov. 18, 1992; revision received May 12, 1993; accepted for publication June 5, 1993.

*Staff Engineer, Flight Operations, 1700 Old Meadow Road. Associate Fellow AIAA.

Introduction

THE GSTAR and SPACENET satellites are momentum-biased RCA Series 3000 communication satellites, operating in the geosynchronous orbit. The attitude control system uses three-axis attitude control techniques.[1,2] A momentum level of 475 in-lb-s is provided by a momentum wheel assembly (MWA), with the momentum wheels nominally spinning at 6000 rpm along the pitch axis. The MWA also facilitates full three-axis control by providing the gyroscopic stiffness of the wheel axis in inertial space and its servo-controlled exchange of angular momentum with the spacecraft body. The pitch axis is continuously aligned along the orbit normal by onboard magnetic torquers, thereby providing the roll and yaw control.

The dominant source of environmental attitude disturbance on geosynchronous satellites is the solar pressure, as aerodynamic and magnetic torques become less significant with increasing altitude. The gravity gradient torque is also negligible because of the altitude and the symmetrical design of the satellite (Fig. 1). The disturbance resulting from thermal radiation out of the satellite is also considered negligible for these Series 3000 satellites.

The solar pressure forces and torques depend upon the particular spacecraft configuration and the optical properties of its surface materials. This paper investigates the actual disturbance torque experienced by the satellites as deduced from the control system performance available from the flight data, and is a reduced version of Ref. 3, which was a more detailed presentation of on-orbit data.

Solar Radiation Pressure

Electromagnetic radiation results in radiation pressure on a surface normal to the direction of propagation. The forces and

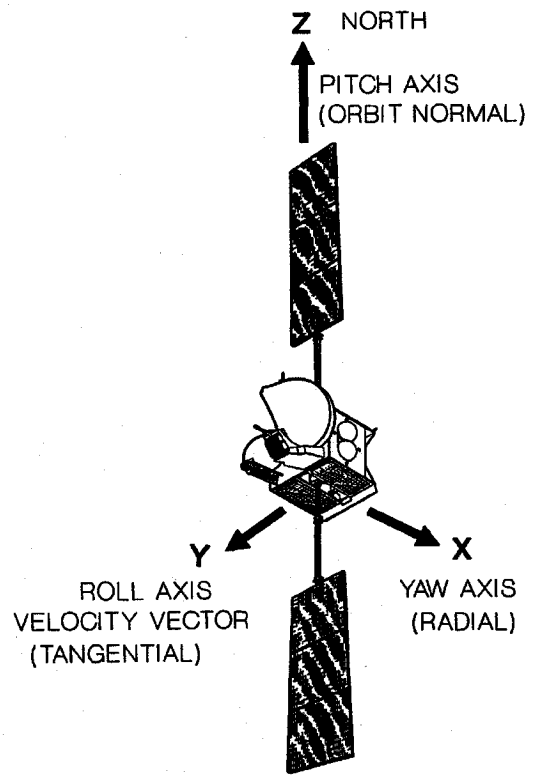

Fig. 1 SPACENET communication satellite.

torques exerted on the satellites by the solar radiation pressure depend on the configuration geometry, nature of the surface, solar ray incidence angle, and the distance from the sun.

A surface will absorb a fraction, α, of the incident ray, specularly reflect a fraction, ρ_s, and diffusely reflect a fraction ρ_d. The sum of these is equal to the total incident energy:

$$\alpha + \rho_s + \rho_d = 1$$

The elementary force on the elementary area dA_r, assuming Lambertian diffusion is

$$d\bar{F} = P_0 dA_r \left[\hat{s}\alpha\,(\hat{s}\cdot\hat{n}) + 2\hat{n}\rho_s\,(\hat{s}\cdot\hat{n})^2 + \rho_d\,(\hat{s} + \tfrac{2}{3}\hat{n})\,(\hat{s}\cdot\hat{n})\right]$$

This elementary force integrated over the illuminated portion of the vehicle surface provides the total solar force acting on the vehicle.

The translational effect of this solar force is to distort the satellite orbit by providing an acceleration along the sun ray. This has the largest long-term effect on the eccentricity of the orbit[4], particularly for satellites with a large area-to-mass ratio.

The elementary torque on the vehicle due to the illumination of the surface dA_r is

$$d\bar{T} = (\bar{r} - \bar{r}_c) \times d\bar{F}$$

This elementary torque integrated over the illuminated portion of the vehicle will give the total torque acting on the vehicle.

The manufacturer of GSTAR and SPACENET satellites had provided a prediction of the expected solar radiation torque, based on the previously given computations. The solar arrays and the satellite body had been modeled as approximately 50 different surfaces and the net torque calculated. A P_0 value of 9.85×10^{-8} lb/ft^2 was assumed, while the values for α, ρ_d, and ρ_s were assumed to be 0.8, 0.1, and 0.1 for solar arrays, and 0.35, 0.325, and 0.325 respectively for most of the other surfaces. The values so obtained are noted in the appropriate sections of this paper for comparison with the computed on-orbit disturbances.

Pitch Control System

In the presence of environmental (solar) disturbances, the pitch control loop of the attitude control system (ACS) maintains the Earth orientation of the satellites about the pitch axis. The Earth is sensed by the Earth sensor assembly (ESA) and this information is used in the feedback loop to provide a servo-controlled exchange of angular momentum between the MWA and the spacecraft main body to maintain the desired pitch pointing. The rate of change of wheel speed is proportional to the magnitude of the disturbance.

When the MWA speed reaches a saturation threshold (6000 $\pm$ 200 rpm), pitch control thrusters are fired to bring the wheel speed back to the nominal 6000 rpm. During maneuvers, pitch control thrusters are activated to augment the pitch control torque provided by the MWAs.[5]

Pitch Disturbance Torque

The MWA is effectively a mechanical integrator of the pitch torque. Therefore, differentiating the MWA speed profile over a 24 h period yields the pitch torque profile.

The wheel speed profile is primarily a cycle over a day, with a secular component. The cyclic profile results from the solar pitch torque generated as the satellite rotates about its pitch axis once in 24 h. The net change in wheel speed over a 24 h period results from secular component of solar torque, and it accumulates over several days and makes the wheel speed approach a momentum saturation limit. Momentum unload thrusters have to be activated periodically to bring the wheel speed back to its nominal value.

Both the magnitude of the cycle and the net secular variation result from solar radiation applying a pitch torque on the satellite. The pitch torque would therefore be dependent on the declination of the sun, the shape and profile of the satellite, and the optical properties of the satellite surface. The radiation level of the sun is also a factor in the pitch disturbance torque.

Seasonal Effects

Figures 2 and 3 show the wheel speed change over a day on SPACENET I and GSTAR I, respectively. The plots correspond to sun position at vernal equinox, summer solstice, autumnal equinox, and the winter solstice. The effect of the sun's declination on the wheel speed change is apparent, although the two satellites have differing responses caused by differences in mass, surface properties, and the surface profiles. During the 1990–1991 timeframe, the net wheel speed change in SPACENET I and GSTAR I is seen to be negative at all times, with the maximum secular change in autumn, and the minimum in summer. In summer, an occasional reversal in net wheel speed change over a day has also been experienced. Differentiating the wheel momentum profile over a day provides

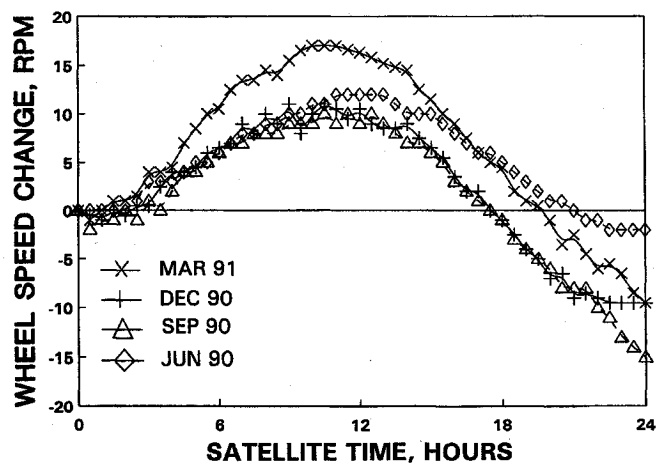

Fig. 2 SPACENET I wheel speed change over a day.

the corresponding solar pitch torque profile. The truncated Fourier series coefficient of this torque for SPACENET I and GSTAR I is given in Tables 1 and 2. This may be compared with the manufacturer's prediction of body fixed pitch torque 1.25×10^{-5} in-lbf, and an inertially fixed torque of 3.7×10^{-5} in-lbf as the maximum under normal operating conditions.

As previously stated, the declination of the sun is the primary reason for the differing wheel speed profile. However, the large difference in the pitch torques corresponding to the two equinoxes (sun declination is zero), for both GSTAR I and SPACENET I, indicates that sun declination is only one of the factors.

Effects of Change in Mass Property

The torque produced by the solar pressure is dependent on the moment arms of each of the incident surfaces, and therefore is dependent on the center of mass of the satellites. The center of mass varies with propellant depletion over the lifetime of a satellite. In addition, the optical and structural properties of the satellite surface, of the solar arrays in particular, also degrade over time. Reference 5 indicated a noticeable bending of the solar arrays in the direction of the sun, and this deflection increases with time.

The combined effects of this gradual change in satellite mass and structure result in the changing nature of the pitch disturbance torque and related wheel speed changes. Figure 4 shows the SPACENET I wheel speed trend in 1984–1985 and Fig. 5 shows the GSTAR I wheel speed trend in 1985–1986.

The trend of the pitch torque towards the satellite's end of life has been predicted in Ref. 3. The expected trend is a net positive secular change in wheel speed for most of the year. This indicates a reversal in solar pitch torque with depletion of propellant.

Diurnal Variation in the Satellite's Center-of-Mass

A large offset in center-of-mass location results in the large amplitude of the cyclic pitch torque as the satellite rotates about its pitch axis. However, the cause of the large secular component of pitch torque on a primarily symmetric satellite is not apparent. A partial explanation is the diurnal variation in the center-of-mass location.

This daily variation is different from the gradual change that results from propellant depletion. Its cause is the daily fluctuation in temperature in each of the tanks that results in the transfer of some amount of propellant between tanks. The propellant (hydrazine) and pressurent (helium) are stored in the

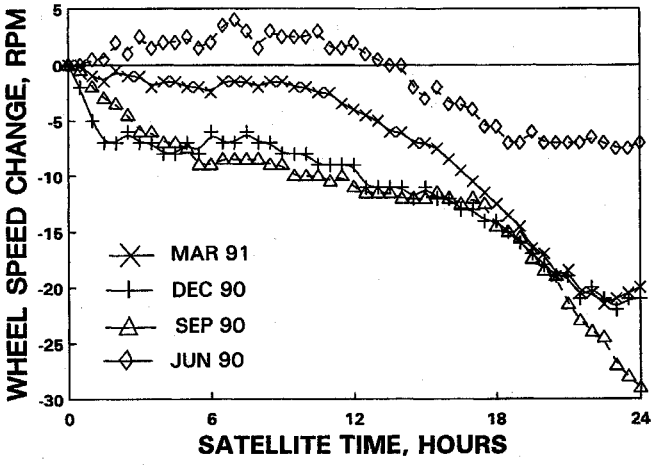

Fig. 3 GSTAR I wheel speed change over a day.

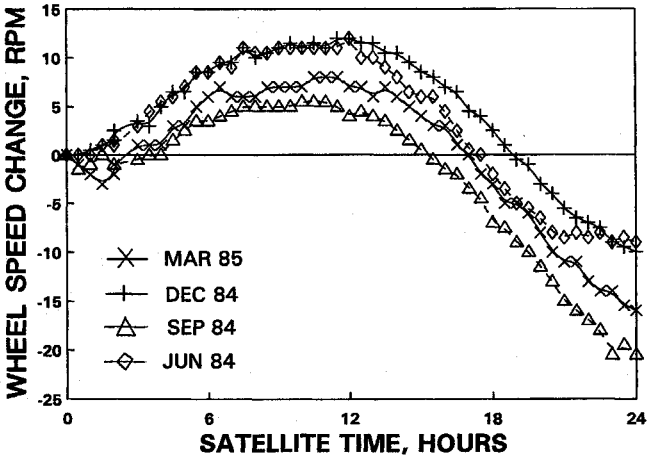

Fig. 4 SPACENET I wheel speed change over a day in 1984–1985.

Table 1 SPACENET I pitch disturbance torque in 1990/1991 (in-lb)

Fourier coefficient[1]	June, 1990	Sept. 1990	Dec. 1990	March 1991
a_0	-1.3×10^{-6}	-1.1×10^{-5}	-8.5×10^{-6}	-8.0×10^{-6}
a_1	3.2×10^{-6}	9.7×10^{-6}	-1.6×10^{-6}	8.0×10^{-6}
b_1	3.8×10^{-5}	5.0×10^{-5}	5.1×10^{-5}	5.5×10^{-5}
a_2	-1.5×10^{-6}	2.3×10^{-6}	9.0×10^{-7}	6.9×10^{-6}
b_2	-1.6×10^{-6}	-1.1×10^{-5}	5.4×10^{-7}	-5.8×10^{-6}
a_3	2.1×10^{-7}	-6.7×10^{-6}	-1.0×10^{-6}	-6.1×10^{-6}
b_3	4.6×10^{-6}	1.1×10^{-5}	-1.8×10^{-6}	8.3×10^{-6}

[a]The disturbance torque is expressed by: $\tau = a_0 + a_1 \cos(\beta) + b_1 \sin(\beta) + a_2 \cos(2\beta) + b_2 \sin(2\beta) + a_3 \cos(3\beta) + b_3 \sin(3\beta)$ where: β = orbit o'clock angle, where 0 deg is spacecraft midnight.

Table 2 GSTAR I pitch disturbance torque in 1990/1991 (in-lb)

Fourier coefficient	June, 1990	Sept. 1990	Dec. 1990	March 1991
a_0	-5.7×10^{-6}	-2.7×10^{-5}	-2.0×10^{-5}	-1.7×10^{-5}
a_1	2.0×10^{-5}	-2.3×10^{-5}	-5.7×10^{-6}	6.4×10^{-6}
b_1	1.3×10^{-5}	1.3×10^{-5}	1.6×10^{-5}	1.8×10^{-5}
a_2	-4.5×10^{-6}	3.4×10^{-6}	2.8×10^{-6}	-7.9×10^{-6}
b_2	-1.3×10^{-6}	-8.5×10^{-6}	-5.7×10^{-6}	1.6×10^{-6}
a_3	-3.0×10^{-6}	9.2×10^{-6}	-4.0×10^{-8}	2.7×10^{-6}
b_3	-3.2×10^{-6}	-5.0×10^{-6}	-7.0×10^{-6}	6.5×10^{-6}

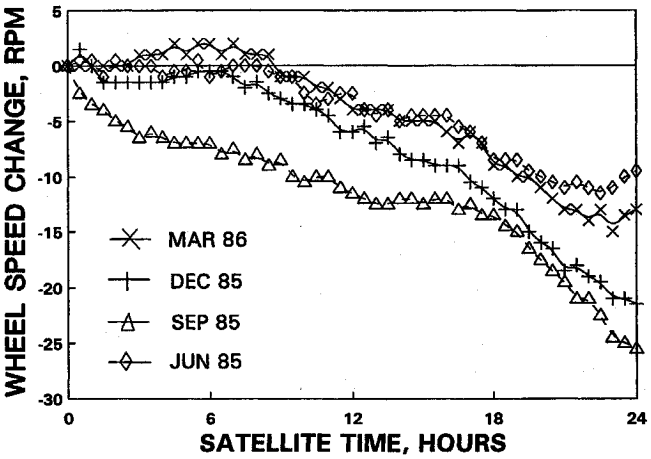

Fig. 5 GSTAR I wheel speed change over a day in 1985–1986.

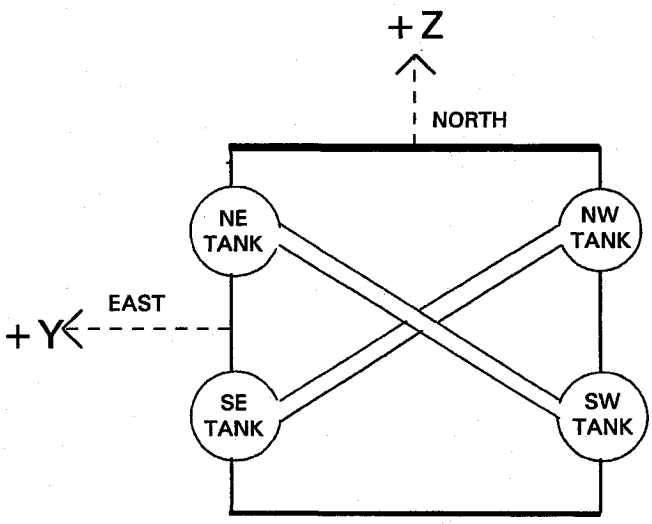

Fig. 6 Propellant tank locations.

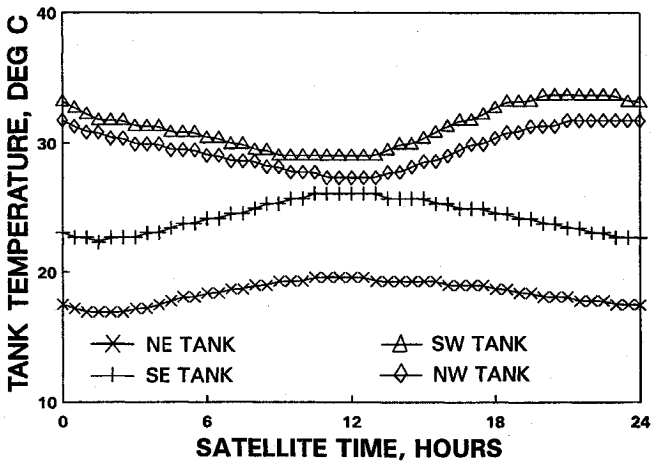

Fig. 7 SPACENET I tank temperatures in March 1990.

satellites in four tanks, as shown in Fig. 6. This figure also shows the relative location of the propellant tanks in the *Y-Z* plane (the satellite is spinning about the *Z* axis once per day). The interconnected northeast and the southwest tanks supply the odd half propulsion system which consist of eight thrusters (odd numbered), while the northwest and southeast tanks supply the even half, which consists of the remaining eight thrusters (even numbered). Part of each of the tank sphere projects out of the satellite side, and can be directly exposed to the sun.

Figure 7 shows the temperature of all four propellant tanks on SPACENET I during an equinox period. There are three primary contributors to the tank temperature profiles: the proximity of the individual tanks to heat dissipating payloads, the declination of the sun, and the daily rotation of the tanks about the satellite pitch axis. In addition, the amount of propellant in each half system would also affect the temperature reading, provided there is enough propellant to touch the thermistor. At equinoxes (sun 0 deg declination) there is no differential solar radiation on the individual tanks; therefore, Fig. 7 indicates that the southwest and the northwest tanks are the warmest because those panels have the maximum payload heat dissipation, and the northeast panel has the minimum amount of heat dissipation. Superimposed on the temperature curve of each tank is a cycle of approximately 5° amplitude, resulting from the varying solar radiation as the tanks rotate about the pitch axis.

Reference 3 has the tank temperature trends for all seasons, and discusses the effect of sun declination on tank temperatures. In summer, the north tank temperatures are relatively elevated, while in winter, the south tank temperatures are higher.

As the four tanks undergo a temperature cycle on a daily basis, the connected tank temperatures (NE-SW and NW-SE) also cycle relative to each other, with the closest approach around satellite noon. The odd half system had approximately 12 kg more propellant than the even half, resulting in a larger temperature variation between the two connected tanks, as explained earlier. Because of this temperature gradient some amount of propellant is expected to be pushed from the hotter tank to the cooler one to maintain equilibrium pressure. A sizeable shift of propellant results in a shift in the spacecraft center-of-mass. In the course of the day, propellant will be transferred between the two tanks roughly proportional to the temperature variation which results in a bias of the center-of-mass away from the sun. In the body-fixed coordinates, the center-of-mass will vary primarily along the *X*-axis in a cyclical form. This diurnal shift in center-of-mass is a contributor to the secular pitch torque.

Roll/Yaw Control System

As stated earlier, the SPACENET and GSTAR satellite control system uses the single pitch axis momentum wheel in conjunction with a magnetic roll/yaw control to provide three-axis attitude control. The roll/yaw control is provided by body-mounted electromagnetic torquers whose magnetic dipole interact with the local geomagnetic field, which is properly directed to reduce both roll and yaw attitude errors.

The magnetic torquer is a 150-ampere-turn-meter^2 (Atm^2) electromagnet which is mounted in the main structure of the spacecraft. The control loop attitude reference is obtained from the roll channel of the Earth sensor assembly (ESA), with the gyroscopic coupling of the momentum-bias design removing the need for yaw attitude sensing. The proper dipole moment to reduce both roll and yaw is obtained by appropriately skewing the torquer with respect to the roll axis. The control system implements a bang-bang control function with a selectable deadband (normally 0.01°) and hysteresis is provided to minimize the switching. Ref. 6 has described in detail the design basis of this magnetic control system. It has also been summarized in Ref. 3.

Spacecraft Roll/Yaw Dynamics and Torquer Control

The general equations of roll and yaw motion for a bias momentum satellite can be expressed as[6]:

$$\left[\phi(t) - \frac{T_3}{\omega_0 H}\right] = \left[\phi(0) - \frac{T_3}{\omega_0 H}\right] \cos \omega_0 t - \left[\psi(0) - \frac{T_0}{\omega_0 H}\right]$$

$$\sin \omega_0 t + \frac{1}{2\omega_0 H}[(T_1 + T_5) + (T_2 + T_4)\,\omega_0 t] \sin \omega_0 t$$

$$+ \frac{1}{2\omega_0 H}(T_1 - T_5)\,\omega_0 t \cos \omega_0 t$$

$$\left[\psi(t) - \frac{T_0}{\omega_0 H}\right] = \left[\psi(0) - \frac{T_0}{\omega_0 H}\right] \cos \omega_0 t + \left[\phi(0) - \frac{T_3}{\omega_0 H}\right]$$

$$\sin \omega_0 t + \frac{1}{2\omega_0 H}[(T_2 - T_4) + (T_1 - T_5)\,\omega_0 t] \sin \omega_0 t$$

$$- \frac{1}{2\omega_0 H}(T_2 + T_4)\,\omega_0 t \cos \omega_0 t$$

To control the disturbance torque, roll/yaw torque is applied when the roll threshold is exceeded. For SPACENET and GSTAR satellites, a roll threshold of 0.01 deg is used. As explained in Ref. 6, although the torquer is activated based on the roll error signal only (there is no yaw error data in normal operational mode), with an optimum alignment of the torquer (skew angle α_s) both roll and yaw error are reduced. However, the yaw reduction is not as efficient as the roll control, and typically the yaw error would be five times the roll error.

When torquer control is applied, the given equations would still be valid under the condition that $T_0 = MB\cos\alpha_s + k_0$ and $T_3 = MB\sin\alpha_s + k_2$.

Table 3 provides the details of the magnetic torquers and computes the maximum body fixed roll and yaw control torques provided by the torquers (neglecting the diurnal variation in geomagnetic field), for both SPACENETs and GSTARs.

Solar Arrays and Inertial Torque

Solar arrays, with a combined surface area of 153 ft^2 provide the biggest surface for the solar radiation pressure. The solar disturbance torque is, however, kept to a minimum because of the symmetric arrangement of the arrays (Fig. 1) and because the solar array axis passes as close to the spacecraft center-of-mass as possible.

Solar arrays are the primary source of inertially fixed solar torque on the satellites. The varying declination of the sun, the bending of the array surfaces, and the fact that the array normal is ahead of the sun by about 35–50 deg due to excess array power capacity, all create the inertial disturbance.

For the current satellite designs torquer control has to be augmented by differentially slewing the north array with respect to the south to provide a propeller torque, to provide an inertially fixed torque to counteract the disturbance torque, provided the phasing is correct.

The phenomenon of solar-induced propeller torque, which has a large contribution to the environmental disturbance and its control, has been discussed in some details in Ref. 3. It also has the computed magnitude and phase of the propeller torque for different combinations of array angles and offsets.

The slewing of the north array relative to the south on a regular basis provides the relative offset δ, and Fig. 8 provides a slew history over a year for both SPACENET I and GSTAR I satellites. The difference in δ, noted in Fig. 8, between structurally similar satellites is probably due to differing amounts of built-in misalignment between arrays, solar array bending for different satellites, and optical degradation of the array surfaces.

Table 3 Magnetic control torque

M:	150 Atm^2
i:	11.4 deg
R_m:	1.066×10^{-7} webers/m^2
A:	0.15 zero to peak
α_s:	59.1 deg SPACENET
	51.8 deg GSTAR
Available control torque (in-lbf):	
SPACENET:	1.19×10^{-4} (roll)
	7.12×10^{-5} (yaw)
	1.09×10^{-4} (roll)
GSTAR:	8.58×10^{-5} (yaw)

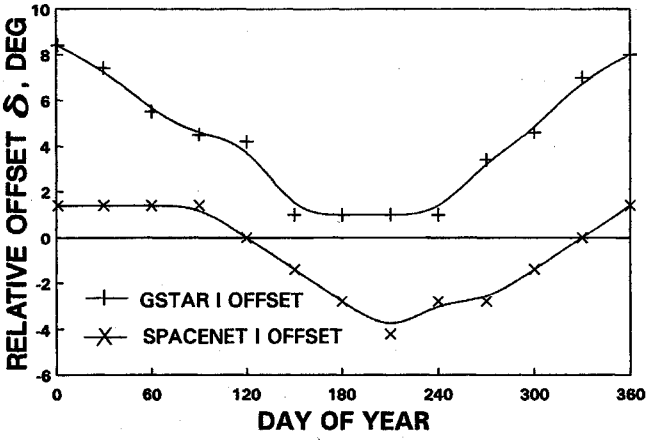

Fig. 8 Relative offset between north and south array over a year.

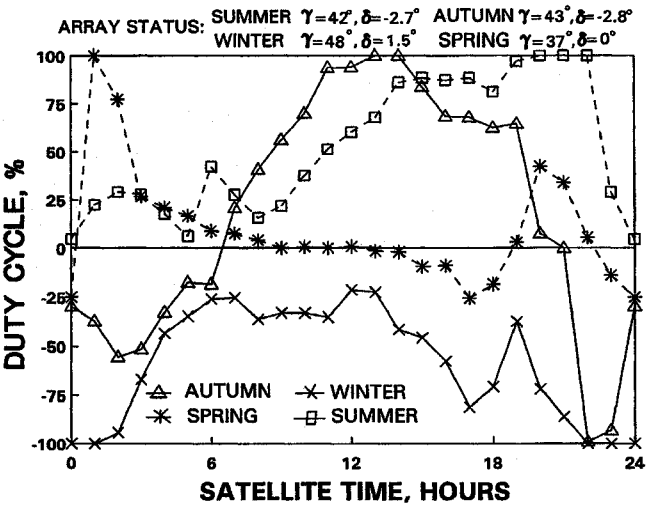

Fig. 9 SPACENET I torquer duty cycle.

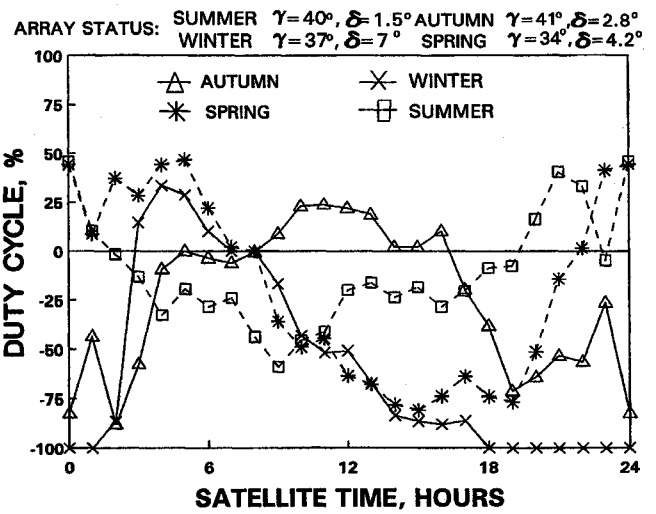

Fig. 10 GSTAR I torquer duty cycle.

Seasonal Effects on Roll/Yaw Torque

Since the disturbance torque is caused by the solar radiation pressure, the declination of the sun is the biggest factor in the seasonal variation of the roll and yaw torque. The changes are reflected in the amount of relative array offset and the nature of torquer activity. The seasonal variation in the array offsets have been described in the above section and are noted in Fig. 8. Figures 9 and 10 show the seasonal variation in torquer

activity for the two satellites. The plots correspond to the time around the respective solstices and equinoxes.

SPACENET I is relatively symmetric in its seasonal behavior, as reflected in the nature of relative array slews as well as the torquer duty cycles. During the equinoxes, the torquers operate in both the positive and negative range over a day, although the signatures are different for the two equinoxes (Fig. 9). This difference is probably the result of the hysteresis effect of the inertial torque provided by the arrays. The torquer operates entirely in the positive region during the summer solstice, and entirely in the negative range during the winter solstice. The torquers are more likely to saturate (operate at 100% duty cycle) for a part of the day during the solstices. During such periods, the roll error tends to exceed the torquer threshold of 0.01 deg, and arrays need to be trimmed to assure that the roll excursions do not exceed the operating specifications. GSTAR I is relatively asymmetric in its seasonal behavior. During the equinox periods (Fig. 10), the torquers operate in both the positive and negative ranges. During the summer solstice, however, the torquer does not remain exclusively in the positive operating region as in SPACENET I. During the winter solstice, the torquers are primarily in the negative operating region, and despite the large offset of 7 deg in solar arrays, the torquers stay at 100% duty cycle for a relatively large part of the day. It is primarily in winter that the roll errors frequently exceed the magnetic control threshold of 0.01 deg and the arrays have to be adjusted very frequently to control the roll.

Roll/Yaw Disturbance Model

The effects of roll and yaw torque are absorbed by a combination of the torquers, the solar array offset, and by actual precession of the satellite momentum vector resulting in actual roll and pitch error. Unlike the pitch disturbance torque, which only affects the MWA wheel, and therefore can be determined by analyzing the wheel performance, the roll and yaw torque is not directly observable from torquer activity. Some of the constraints in doing this are:

1) The torquer design involves one torquer affecting both roll and yaw torque, while being activated on roll error alone. In addition, the torquer dead-band and the associated delay logic provide nonlinearity in torquer operation. This makes it difficult to determine the disturbance from torquer duty cycle.

2) When the torquer duty cycle reaches 100%, any more solar radiation torque results in actual precession of the satellite momentum vector, resulting in satellite roll and yaw. There is no independent yaw sensor (yaw is controlled by its coupling into roll over a 6 h period), and the actual amount of precession resulting from the radiation pressure cannot be computed.

An adequate method of computing the actual roll and yaw disturbance would be using detailed simulation models and matching the simulated torquer data resulting from assumed disturbance models with the actual torquer data from the operational satellites.

The roll and yaw disturbance computed for this paper have been obtained by making a simple model of the satellite dynamics and torquer control, and matching the simulated torquer data resulting from an assumed disturbance model with the actual torquer and roll angle data (Figs. 11 and 12). This simple model provides some basic characteristics of the roll and yaw disturbance torque acting on the GSTAR and SPACENET satellites, as well as its secular and seasonal variations.

An attempt is made to match the torquer duty cycles shown in Figs. 9 and 10, using a very simplified disturbance model, consisting of only the a_0, a_1, and the b_1 terms of Fourier series. Using more terms would not necessarily increase the accuracy of the results due to the simplified nature of the torquer/dynamics model itself. Tables 4 and 5 show the results thus obtained, and these represent a reasonably good match in magnitude, and an approximate match in phase of the disturbance torques. As an example, Fig. 12 is an attempt to match the actual torquer and attitude history of SPACENET I during the winter solstice (Fig. 11). The plots show an approximate match, and a more

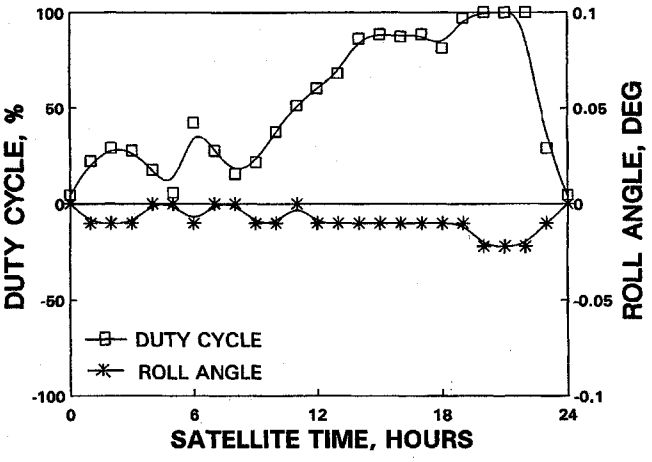

Fig. 11 Actual SPACENET I torquer duty cycle and roll angle, winter solstice.

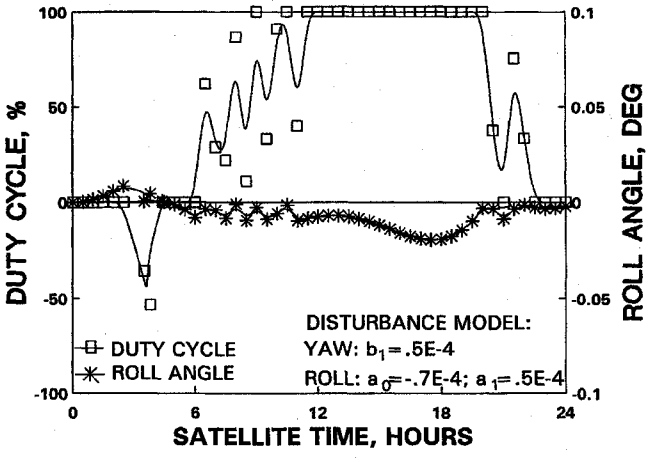

Fig. 12 Simulated torquer duty cycle and roll error.

sophisticated model of the torquer/spacecraft dynamics would result in a much better fit. The torque coefficients noted in Table 4 were used for the disturbance torque models.

It may be noted that under normally operating conditions, the maximum yaw disturbance torque predicted by the manufacturer was 0.55×10^{-5} in-lbf in body-fixed torque, and 0.15×10^{-4} in-lbf in inertially fixed torque, while the roll disturbance predicted was 0.1×10^{-4} in-lbf in body-fixed torque and 0.15×10^{-4} in-lbf in inertially fixed torque. As noted in Ref. 3, the roll/yaw torque is very sensitive to the solar array deformations and orientations, relative to both the sun line and to each other. The operational orientations of the arrays vary from the initial design assumptions, and the on-orbit disturbance experienced is substantially larger than the design predictions.

Solar Flux and Geomagnetic Storm

The solar pressure disturbance analyzed so far is for a nominal level of solar activity. The disturbance torque on all axes is very much affected by the activities on the sun that result in solar flares and geomagnetic storms. During such occurrences, the roll/yaw attitude of the satellite cannot be controlled by the magnetic torquers, and roll control thrusters are needed to augment the control.

The mechanics of this disturbance is the geomagnetic storm resulting from solar activity. Portions of solar wind's energy is transferred to the magnetosphere, causing Earth's magnetic field to change rapidly in both direction and intensity.[7,8] The onboard magnetic torquers respond to this activity, causing the attitude disturbance. Fig. 13 shows a clear relationship between the planetary magnetic activity index (*ap*) and the pitch torque, as indicated by the change in the MWA speed. During magnetic

Table 4 Computed SPACENET I roll/yaw disturbance

Disturbance	Fourier[a] coefficient	Vernal equinox	Summer solstice	Autumnal equinox	Winter solstice
Yaw torque (in-lbf)	a_0	0	0	0	0
	a_1	−0.3*E*-4	0	0.5*E*-4	0.3*E*-4
	b_1	0	0.5*E*-4	0	0
Roll Torque (in-lbf)	a_0	−0.3*E*-4	−0.7*E*-4	0	0.6*E*-4
	a_1	0	0.5*E*-4	0	0
	b_1	0.3*E*-4	0	−0.5*E*-4	−0.3*E*-4

[a]The disturbance torque is expressed by: $\tau = a_0 + a_1 \cos(\beta) + b_1 \sin(\beta)$ where: β = orbit o'clock angle, where 0 deg is spacecraft midnight.

Table 5 Computed GSTAR I roll/yaw disturbance

Disturbance	Fourier coefficient	Vernal equinox	Summer solstice	Autumnal equinox	Winter solstice
Yaw torque (in-lbf)	a_0	0	0	0	0
	a_1	−0.4*E*-4	−0.3*E*-4	0.3*E*-4	0.55*E*-4
	b_1	0	0	0	0
Roll torque (in-lbf)	a_0	0.4*E*-4	0.3*E*-4	0.3*E*-4	0.4*E*-4
	a_1	0	0	0	0
	b_1	0.4*E*-4	0.3*E*-4	−0.3*E*-4	−0.55*E*-4

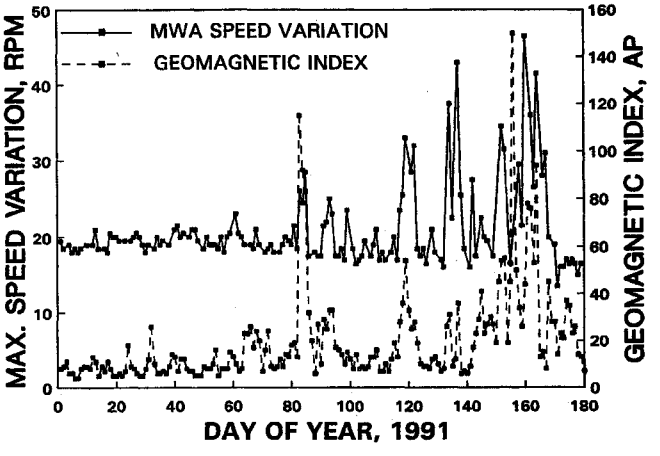

Fig. 13 Effect of geomagnetic activity on SPACENET I wheel speed change.

storms, it is often beneficial to turn the magnetic torquers off to make the satellite less susceptible to the magnetic disturbance.

Conclusion

This paper has analyzed the on-orbit satellite control system performance to determine the environmental disturbances to which the GTE SPACENET and GSTAR series of communication satellites are subjected. In geostationary orbit, the primary source of disturbance is the solar radiation pressure.

Analysis of the momentum wheel performance provides insight into pitch disturbance torque. Data has shown that this disturbance is correlated to the declination of the sun. It also depends upon the year of satellite life, implying the variance of mass properties of the satellite with time. On a shorter time frame, gradients in propellant temperature cause the center-of-mass to migrate on a daily basis, providing a perturbation in the pitch torque. As can be expected, there is a strong correlation between the solar flux and the disturbance torque.

Analysis of the magnetic torquer activities, along with the relative solar array offsets and roll/yaw error provided an estimate of the roll and yaw solar torque. This had to be indirectly estimated by assuming a simple model of the satellite dynamics and torquer logic and matching the results with the actual data.

This paper has identified the actual solar pressure torque acting on the satellites. Further work needs to be done to identify the different parts of the satellite that cause the different disturbance signature. This will require making a full-fledged model of the satellite surfaces and identifying the resulting solar pressure torque from all the surfaces.

In addition, by tracking the change in satellite disturbance over time, it might be possible to isolate the effects due to changes in mass properties from changes in optical/thermal properties of the satellite surfaces, and thereby discern a trend in the respective change or degradation over time. Data provided in this paper should be useful for satellite operations where the empirical data may be used to preplan and optimize attitude control activities. In addition, this data should also provide the satellite designers the opportunity to validate and/or update the solar pressure disturbance models that are used to design the attitude control systems. It has been noted that the actual disturbance experiences on orbit are larger than the design prediction.

References

[1] Muhlfelder, L., "Developments in Attitude Control Systems at Astro-Electronics," *RCA Technical Communications,* 1978, pp. 81–90.

[2] Keigler, J. E., Lindorfer, W. J., and Muhlfelder, L., "Stabilite Attitude Control for Synchronous Communication Satellites," AIAA Paper 72-572, April 1972.

[3] Parvez, S. A., "Solar Pressure Disturbance on GSTAR and SPACENET Satellites," AIAA Paper 92-4335, Aug. 1992.

[4] Kamel, A. A., and Wagner, C. A., "On the Orbital Eccentricity Control of Synchronous Satellites," *Journal of the Astronautical Sciences,* Vol. 30, No. 1, 1982, pp. 61–73.

[5] Parvez, S. A., "GSTAR Satellite Disturbance from Plume Impingement," *Journal of Spacecraft and Rockets,* Vol. 27, No. 3, 1990, pp. 275–278.

[6] Schmidt, G. E., Jr., "Magnetic Attitude Control for Geosynchronous Spacecraft," AIAA Paper 78-570, April 1978.

[7] Anon., "Introduction to the Space Environment," Space Environment Service Center, National Oceanic and Atmospheric Administration, Boulder, CO, May 1990.

[8] Gourney, D. J., "Solar Cycle Effects on the Near-Earth Space Environment," *Review of Geophysics,* Vol. 28, No. 3, 1990, pp. 315–336.

Alfred L. Vampola
Associate Editor